Influence of coal dust on premixed turbulent methane–air flames

Scott R. Rockwell, Ali S. Rangwala *

Department of Fire Protection Engineering, Worcester Polytechnic Institute, Worcester, MA 01609, USA

ARTICLE INFO

ABSTRACT

This study discusses the design of a new experimental platform, the Hybrid Flame Analyzer (HFA) to measure burning velocity of gas, dust, and hybrid (gas and dust) premixed flames. The HFA is used to analyze a particle–gas–air system of coal dust particles (75–90 μm and 106–120 μm) in a premixed CH_4–air (ϕ_g = 0.8, 1.0 and 1.2) flame. Experimental results show that particles usually increase the turbulent burning velocity. Smaller particle sizes and larger concentrations (>50 g/m^3) increase turbulent burning velocity compared with larger particle sizes and lower concentration ranges. The experimental data is used to develop a correlation similar to turbulent gas flames to help modeling of the complex behavior.

© 2012 The Combustion Institute. Published by Elsevier Inc. All rights reserved.

1. Introduction

Accidental dust deflagrations represent a hazard to both personnel and equipment, in industries that make, transport or use flammable dusts. Table 1 [1] lists a few of the most recent industrial explosions related to dusts. This study focuses on analyzing the risk of such explosions and especially cases caused by mixtures of flammable gases and dusts (hybrid fuels). This explosion often occurs in coal mines which start with a methane air explosion and entrain coal dust as the flame propagates down the mine gallery.

Hybrid flames have been studied by several researchers [2–9], recently reviewed by Eckhoff [10]. Russo et al. [8] and Liu et al. [9] injected a coal dust/methane mixture into a combustion chamber followed by a central ignition. The flame front was visualized using schlieren measurements recorded on a high-speed camera. They found hybrid mixtures of coal dust-methane–air flames show a lower flammability limit than coal dust-flames. The importance of turbulent intensity was highlighted. However, accurate measurement of turbulence was not achieved. Similar observations are noted in most studies owing to the practical difficulties of measuring turbulent intensities and length scales in a constant volume explosion-sphere experiment. The current study uses a tube burner similar to the design by Kobayashi et al. [11] to anchor a steady turbulent particle–gas–air premixed flame. Pittsburgh Seam Coal dust particles (75–90 and 106–120 μm) are used with equivalence ratios of the CH_4–air of ϕ_g = 0.8, 1, and 1.2. Proximate and ultimate analysis of Pittsburg Seam Coal are reported elsewhere [12]. The

influence of particle interacting with a premixed flame at different turbulent intensity levels is examined.

2. Experimental setup

Figure 1 shows a schematic of the experimental set up named Hybrid Flame Analyzer (HFA). It is designed with the ability to control the, turbulent intensity (u'_{rms}), length scale (l_0), particle size (d_{st}), and concentration (λ_{st}) of dust particles to provide a measure of the burning velocity of gas, dust, or hybrid flames.

The parts of the HFA are the dust feeder, the burner test section, an optical system (shadowgraph) to analyze the turbulent flame and an exhaust. The flame is fueled from a particle screw feeding system, and a methane–air mixture via a mass flow controller. The equivalence ratio (Φ_g) of the methane–air flame is maintained at Φ_g = 0.8, 1, and 1.2 to simulate fuel lean, stoichiometric, and fuel rich premixed gas flames. For a given screw speed, the dust feeder is calibrated by collecting the dust at the end of the tube. The collected dust is weighed and a calibration curve is developed. As shown in Fig. 1, a point source of light using a 480 watt projector bulb is placed at the focal point of a biconvex lens (100 mm diameter and 200 mm focal length). This creates a 100 mm diameter test section of parallel light inside the combustion chamber. The parallel light passes through the flame and through a second identical biconvex lens which lessens the diameter of the image. This decrease makes the image small enough to fit on the sensor of a digital single reflective lens camera with a 1–1 macro lens with the focus set to infinity. To lessen the intensity of the coal dust emissions, a short pass filter with a cutoff of 550 nm is placed in front of the camera lens. The turbulent burning velocity is obtained using the flame images.

* Corresponding author. Fax: +1 508 831 5862.
E-mail address: rangwala@wpi.edu (A.S. Rangwala).

Table 1
Recent incidents of industrial dust explosions [1].

Industry type	Fuel	Location	Date	Fatalities
Saw mill	Wood dust	Lakeland Mills sawmill in Prince George, Canada	2012	2
Saw mill	Wood dust	Babine Forest Products in Burns Lake, Canada	2012	2
Powder manufacturer	Iron dust	Hoeganaes Corporation, TN USA	2011	5 (3 Incidents)
Coal mine	Methane & coal dust	Upper Branch mine, West Virginia, USA	2010	29
Coal mine	Methane & coal dust	Pike River, New Zealand	2010	29
Sugar manufacturer	Sugar dust	Imperial Sugar, Port Wentworth, GA	2008	13
Coal mine	Methane & coal dust	KY, USA	2006	5
Plastics manufacturer	Plastic dust	North Carolina, USA	2003	8
Rubber recycling plant	Rubber dust	Rouse Polymerics International Inc., Vicksburg, MS	2002	5
Powerhouse	Coal dust	Ford Motor Company, Rouge Complex, Dearborn, MI	1999	6
Shell mold manufacturing	Phenol formaldehyde resin	Jahn Foundry, Springfield MA	1999	3
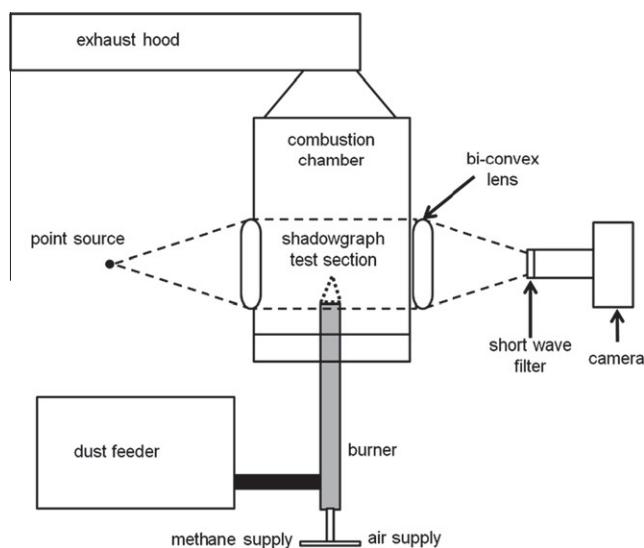
Fig. 1. Experimental setup – Hybrid Flame Analyzer (HFA).
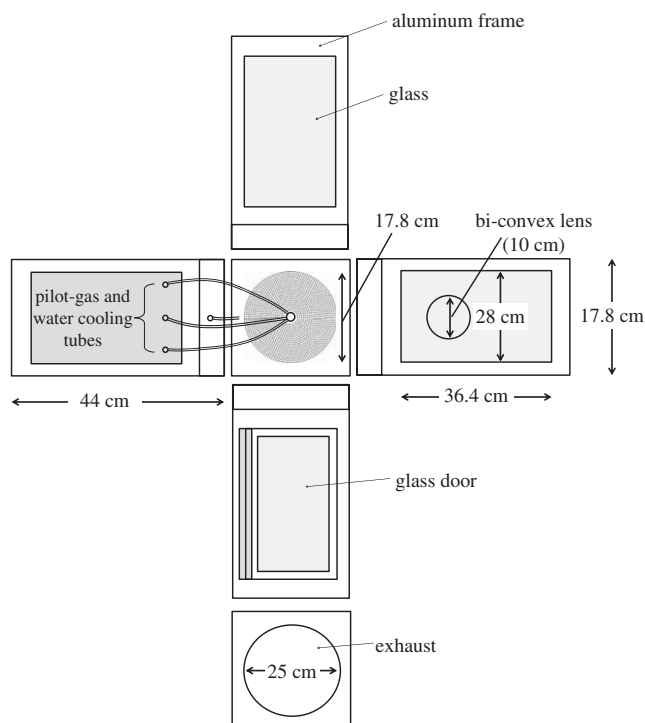
2.1. Combustion chamber

Figure 2 shows the details of the combustion chamber. The external frame is made of aluminum (0.3 cm thick) with dimensions 44 cm tall and 18 cm wide. Two of the walls are made of plate glass for ease of imaging. Water for cooling the burner is injected and removed through two adaptors as shown in Fig. 2. One side of the combustion chamber is a door for easy access. The top of the combustion chamber contains a fume hood to remove combustion products.

2.2. Burner nozzle design

The HFA uses a cylindrical tube burner for burning velocity measurement. Compared with an explosion sphere, turbulent flame anchoring is possible for longer time duration simplifying instrumentation and improving measurement accuracy. This is important because turbulence measurement needs the use of quantities from several time-averaged measurements.

At the top of the vertical feeder tube two different water cooled nozzles, with internal diameters of 14.5 mm, are attached to the top of the feeder tube. The first nozzle is a simple straight tube

Fig. 2. Combustion chamber.
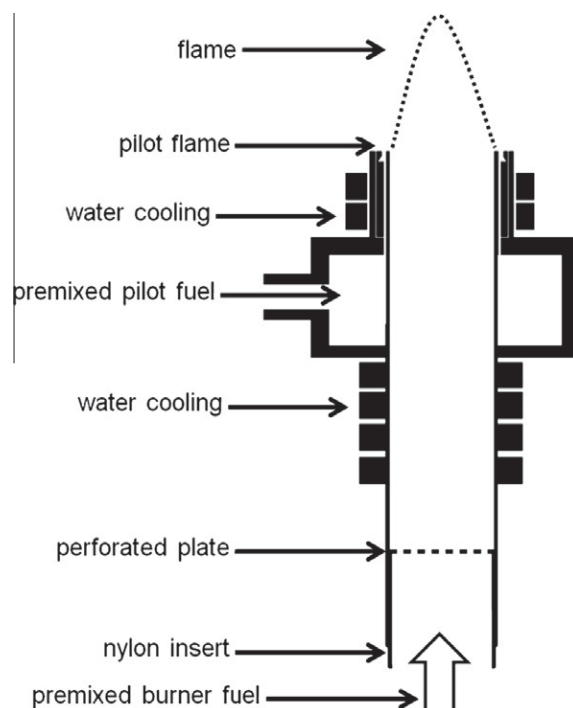
Fig. 3. Turbulent burner nozzle.

Table 2
Flow parameters.

Flow regime	Flow rate (lpm)	Flow velocity (m/s)	u'_{rms} (m/s)	l_0 (mm)	Re
Turbulent	30	3	0.18	1.6	2802
	35	3.5	0.33	1.4	3264
	40	4	0.53	1.1	3736
Laminar	10	1	–	–	926

used for creating laminar flames. The second nozzle uses perforated plates to generate turbulence. It also has a methane-oxygen annular pilot to anchor the turbulent flame.

The details of construction of the turbulent burner nozzle are further illustrated in Fig. 3. The turbulent flame is anchored to the burner nozzle using a methane oxygen pilot flame. A nylon perforated plate, movable within 10–30 mm from the nozzle exit produces turbulence. The blockage ratio of the plate equals 50%. Turbulence intensity control is achieved by adjusting the distance of the perforated plate from the burner exit and the flow velocity. Liu et al. [13] and Roach [14] have shown this to be a reliable way to vary turbulence intensities. Further details are available in Rockwell [15].

The turbulence measurements are performed in cold flow without a flame similar to Kobayashi et al. [11] using a hot-wire anemometer at a sampling rate of 100 kHz. Combined air-methane flow rates of 30, 35, and 40 lpm are used to create turbulent intensities up to 0.532 m/s. Turbulent flow can be described using

$$u = \bar{u} + u', \tag{1}$$

where u is the flow velocity, $\bar{u}$ is the average flow velocity, and u' is the fluctuating component of the flow velocity. The turbulent intensity is defined as the root mean square (RMS) of the turbulent fluctuation in the u' and is calculated using

$$u'_{rms} = \sqrt{\frac{(u'_1)^2 + (u'_2)^2 + \ldots + (u'_n)^2}{n}}. \tag{2}$$

The integral length scale l_0 of the turbulence is calculated using [16]

$$l_0 = \bar{u} \int_0^\infty \rho_u(\tau) d\tau, \tag{3}$$
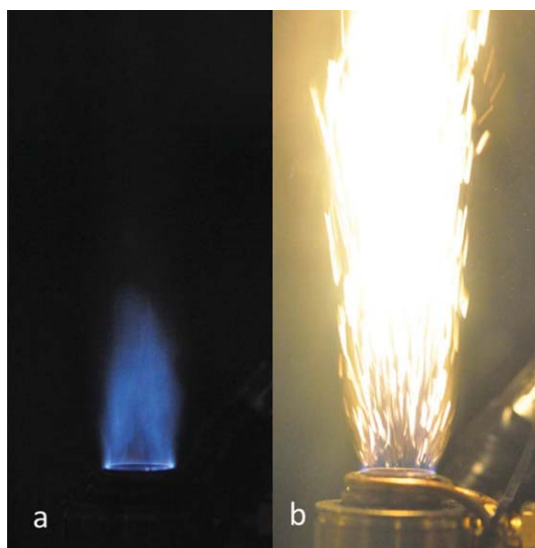
Fig. 4. Visual images of burner flames (a) methane air only ($\phi_g = 0.8$, $u'_{rms} = 0.532$ m/s) (b) hybrid flame including coal dust ($\lambda_{st} = 50$ g/m³, $d_{st} = 75$–90 μm).
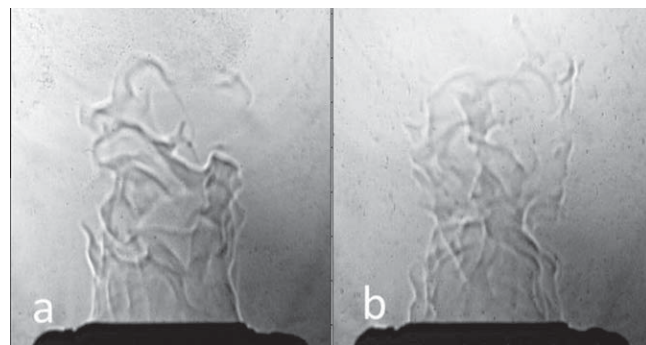
Fig. 5. Shadowgraph images of burner flame (a) methane air only (b) hybrid flame including coal dust ($\lambda_{st} = 50$ g/m³, $d_{st} = 75$–90 μm).

where $\bar{u}$ is the average flow velocity and $\rho_u(\tau)$ is the autocorrelation of the velocity fluctuation. Table 2 shows the various flow parameters measured.

2.3. Image analysis

The HFA uses a shadowgraph to determine the flame edge of the premixed portion of the hybrid flame. For dust-flames the technique is valuable mainly because the flame edge cannot be captured directly as shown in Fig. 4 showing an example of visual images taken of (a) a methane–air flame and (b) a hybrid flame including coal dust. It is clear that the premixed flame edge cannot be determined from visual images. Figure 5 shows shadowgraph images of the same (a) a methane air only flame, and (b) a hybrid flame including coal dust. The flame edges are clear in both cases though in (b) contrast is slightly reduced due to emissions from the coal.

3. Experimental results and analysis

3.1. Burning velocity

The calculation of the turbulent burning velocity in this work is similar to Grover et al. [17] who averaged the measured flame height for several images to determine the burning velocity of a turbulent flame. The method uses,

$$S_T = \bar{u} \sin \alpha, \tag{4}$$

to calculate the burning velocity where $\bar{u}$ is the mean flow velocity and α is the half angle of the right cone with a height equal to the mean flame height.

Figure 6 depicts the procedure adopted. Figure 6a shows a sample shadowgraph image of a methane–air gas flame, with equivalence ratio $\phi_g = 0.8$, and turbulent intensity $u'_{rms} = 0.185$ m/s. The subscript "g" in the equivalence ratio indicates a premixed gas-only quantity. The subscript "st" indicates quantities related to a hybrid mixture. Using a MATLAB program the image is cropped, the blue channel is extracted, the intensity of the image is increased, and the edge of the flame is selected by manually clicking along the edge, shown as a blue line in Fig. 6b. The pixel locations are converted to a distance with 1 pixel being equal to 0.043 mm. This process is repeated 25 times (for 25 different images) and the location of the flame edges are combined as shown in (d) and averaged as shown in (e). The resulting curve is smoothed and the maximum height of the fitted curve is used to calculate the half angle as $\alpha = \tan^{-1}\left(\frac{0.5d}{h}\right)$, where d is the internal diameter of the nozzle exit and h is the mean flame height. Using this procedure, the calculated burning velocities for turbulent methane–air flames match published data as shown in the next section.
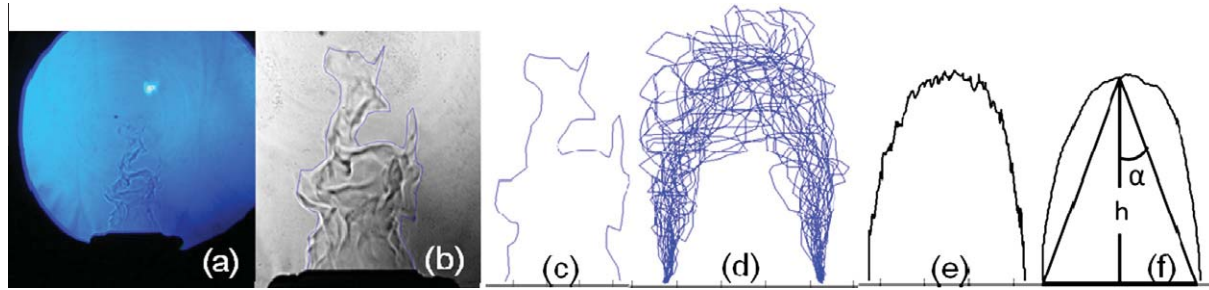
Fig. 6. Turbulent flame image analysis.

3.2. Gas flames (validation study)

To validate the experimental apparatus and procedure the turbulent methane–air flame data is compared with data from published work by Kobayashi et al. [11] as shown in Fig. 7. The turbulent burning velocity $S_{T,g}$ of a methane–air flame ($\phi_g = 1$) is shown vs. turbulent intensity (u'_{rms}). Turbulence is generated using a perforated plate (1 mm hole diameter, blockage ratio of 50%) placed 30 mm below the exit of the nozzle similar to that used by Kobayashi et al. [11]. Error bars, representing the uncertainty in the measurement are one standard deviation of the burning velocity (from 25 images).

Good agreement is observed between the two experimental methods. Similar to Kobayashi et al.'s data the burning velocity increases with turbulent intensity and eventually levels off with high turbulent intensity. Note that Kobayashi et al. used the angle method (c.f. Fig. 3 on pg. 391 of [11]) to extract the turbulent burning velocity from schlieren images of turbulent flames whereas this study uses an alternative method similar to Grover et al. [17] providing similar results.

3.3. Turbulent combustion regimes

Flame images shown in Fig. 5a and b depict how the turbulence influences the reaction zone of a flame. To understand the effect a suitable starting point is to examine the fluid characteristics of the system (cf. Peters [18], Turns [19]). To find out the regime in which the current experiments exist a plot of $\frac{u'_{rms}}{S_L}$ vs. $\frac{l_0}{\delta_L}$ commonly referred to as the Borghi diagram (Peters [18]) is shown in Fig. 8. The regime of the current experiments is within the rectangular shaded region shown in Fig. 8. For the low levels of turbulence created in this work the testing mostly exists in the laminar-flamelet regime. This flamelet regime is divided into the wrinkled and corrugated subsections.
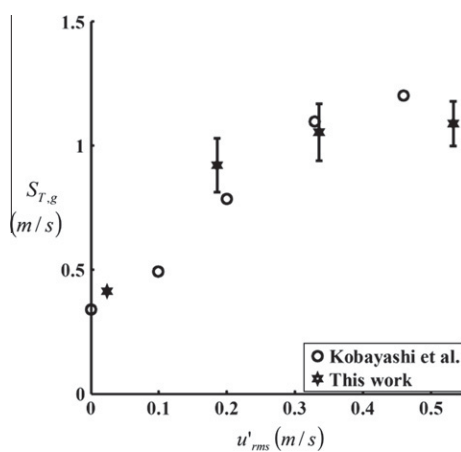
The discussion so far refers to turbulent gas-flames alone. Additional parameters will arise for turbulent dust-flames due to the coupling between the condensed and gas phases. Crowe et al. [20] have shown micron-sized particles influencing the turbulent flow by: (1) displacement of the flow-field by flow around a dispersed phase element; (2) generation of wakes behind particles; (3) dissipation of transfer of turbulence energy to the motion of the dispersed phase; (4) modification of velocity gradients in the carrier flow-field and change in turbulence generation; (5) introduction of additional length scales which may influence the turbulence dissipation; and (6) disturbance of flow because of particle-particle interaction.

Considering fluid mechanics alone (no combustion), additional length scales may also need to be considered. Gore and Crowe [21] have shown that a parameter causing the turbulent intensity to either decrease or increase because of particles in the flow equals d_{st}/l_o, where, d_{st} is the particle diameter and l_o is the integral length scale. When d_{st}/l_o is above ~ 0.07, the presence of particles increases the turbulent intensity. In the current experiments, for the 75–90 μm range, d_{st}/l_o varies between 0.06 and 0.08, while for the 106–125 μm range, d_{st}/l_o varies between 0.07 and 0.11. The particles therefore most likely increase the turbulent intensity in the current experiments. Further, Crowe [22] has shown that the increase in turbulent intensity becomes more pronounced as concentration of particles is increased (c.f. Fig. 3 in [22]).

Fig. 7. Turbulent burning velocity of a methane–air flame (($\phi_g = 1$) vs. turbulent intensity.
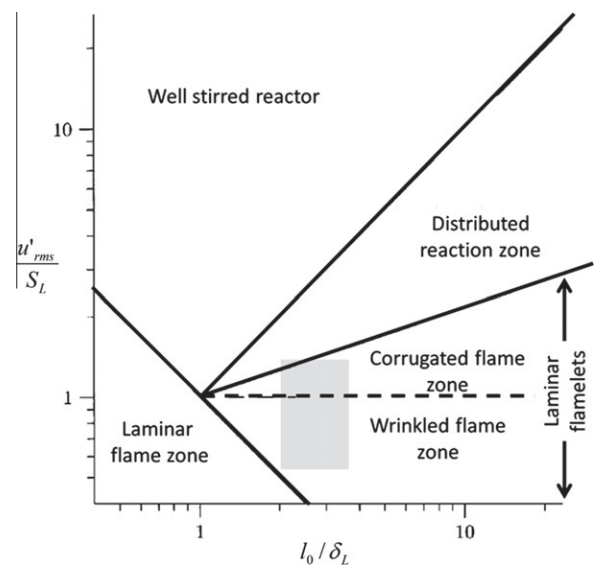
Fig. 8. Characteristic parametric relationships of premixed turbulent combustion. Shaded area depicts current experimental regime.

3.4. Effect of turbulence on burning velocity of a hybrid (dust-CH₄–air) flame

Figure 9a–f show measured turbulent burning velocity for equivalence ratios and particle size ranges tested (λ_{st} represents particle concentration). The laminar burning velocity of the dust-flame ($S_{L,st}$) is used to nondimensionalize the Y-axis. Laminar burning velocity results are reported in an earlier study by Xie et al. [23]. The laminar burning velocity of the gas flame ($S_{L,g}$) is used to nondimensionalize the X-axis. The square connected symbols in Fig. 9 represent the no dust case (CH₄ – air mixture).

In general, Fig. 9 shows the turbulent burning velocity larger than the laminar counter-part for every case studied. The turbulent to laminar burning velocity ratio increases as the turbulent intensity increases for all cases. In cases with smaller particle sizes ($d_{st} = 75 - 90$ μm), as the dust concentration increases beyond 75 g/m³, the ratio of turbulent to laminar flame velocity increases significantly. This is mainly because of the effect of an increase in the turbulence level caused by interacting particles, which also increases with increased number of particles present at higher concentrations [22]. This enhances the overall heat and mass transfer and as a result, the burning velocity increases. While the increasing trend is observed for all three equivalence ratios tested, it is highest for the fuel lean cases since there is also an increase in the local equivalence ratio as discussed recently by Xie et al. [23].

Larger particle sizes (($d_{st} = 106 - 125$ μm) either enhance or dissipate the turbulence. This is also dependent on the size distribution of the particles (mean value of the particle diameter)). Therefore, the combined effects of increase or decrease in the turbulent intensity because of particle injection and the particle size distribution cause a nearly random variation in these cases. However, in this case also, as the intensity increases, the ratio of turbulent to laminar burning velocity increases. An increasing trend with concentration of the dust is also observed, however, only at the higher equivalence ratio of 1.2. Note that for a laminar case, an increase in particle size reduces the laminar burning velocity of a hybrid flame [23,24].

3.5. Correlation of turbulent burning velocity

To find a correlation for the affect of any particular turbulent motion on the turbulent burning velocity a generalized correlation of the form shown in Eq. (5) is used

$$\frac{S_{T,st}}{S_{L,st}} = 1 + C\left(\frac{u'_{rms}}{S_{L,st}}\right)^n, \tag{5}$$

where n is known as the bending exponent and C is a parameter that contains the influence of the scale of turbulence. Figure 10 shows the turbulent burning velocity versus the turbulent intensity. Using Eq. (5), two sets of C and n parameters are found based on fuel
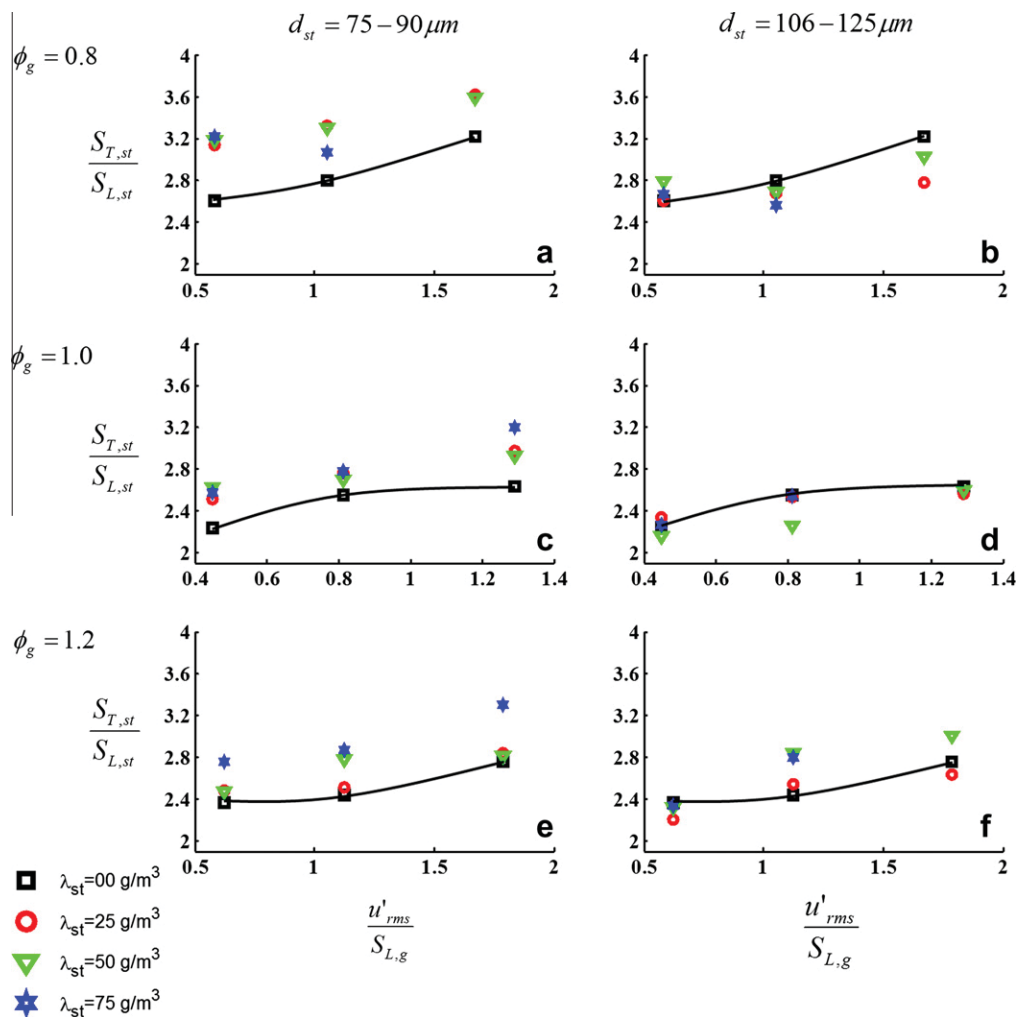
Fig. 9. Turbulent burning velocity vs. turbulent intensity. S_T = turbulent burning velocity and S_L = laminar burning velocity. Subscript "*st*" denotes hybrid mixture and subscript "*g*" denotes premixed gas quantity.
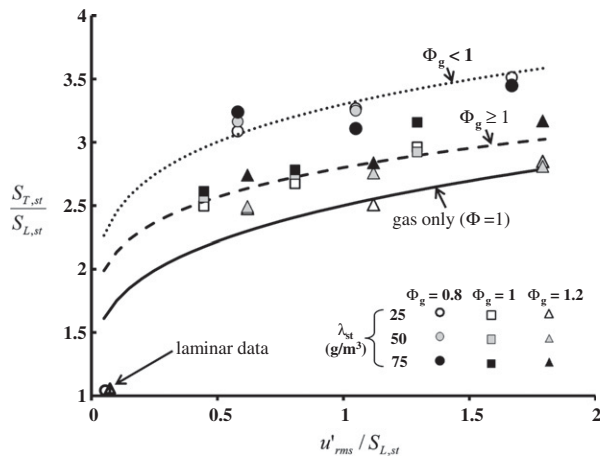
Fig. 10. Correlation for turbulent burning velocity of hybrid flames. Curves represent best fit of experimental data using Eq. (5). Dotted curve, $C = 2.2$, $n = 0.2$, dashed curve, $C = 1.7$, $n = 0.2$ and solid curve, $C = 1.6$, $n = 0.3$. Particle size, $d_{st} = 75$–$90 \ \mu m$.

lean or rich conditions. Two values of C are used because the volatiles release by the dust in the lean phase boost the burning velocity more than with higher equivalence ratios. For gas-phase equivalence ratios less than one the best fit is observed for $C = 2.2$, and $n = 0.2$ (dotted curve in Fig. 10). For equivalence ratios greater than or equal to one, $C = 1.7$, and $n = 0.2$ (dashed curve in Fig. 10). The solid curve in Fig. 10 depicts the gas-only case ($\Phi_g = 1$) or in other words it is the data presented earlier in Fig. 7. In this case, $C = 1.6$ and $n = 0.3$. Since most data-points lie above the solid curve, coal dust particles generally tend to enhance the turbulent burning velocity. For fuel rich flames ($\Phi_g = 1.2$) shown by the triangular symbols in Fig. 10 the turbulent burning velocity of the hybrid dust-flame matches the turbulent burning velocity of a gas flame at $\Phi_g = 1$. However, this only happens at lower dust concentrations. For higher concentrations (>50 g/m³) the presence of dust causes the burning velocity to be higher than that of a stoichiometric gas flame.

A similar plot can also be generated for the larger particle size range tested ($d_{st} = 106 - 125 \ \mu m$). In this case, $C = 2.0$ (fuel lean) and $C = 1.65$ (fuel rich) while the exponent n remains the same ($n = 0.2$). Thus, when particle size range increases a similar trend is observed, although the percentage change in the value of C between fuel lean and fuel rich conditions is smaller when compared with the smaller particle size ranges. This is mainly because of the decrease in the pyrolysis rate of coal dust particles with an increase in diameter.

4. Conclusions

This study develops a new apparatus called the Hybrid Flame Analyzer (HFA) to study premixed turbulent dust-air flames. The HFA is used to study the effect of coal particles on the burning velocity of methane–air flames as a function of particle size, particle concentration, turbulent intensity, and gas phase equivalence ratio. The main conclusions based on the experimental results are:

1. The turbulent burning velocity of methane–air flames increases because of interaction with dust particles (Pittsburgh Seam Coal, 75–90 and 106–120 μm) at turbulent intensities up to 0.532 m/s. The effect is observed for fuel lean, stoichiometric, and rich methane–air flames. A likely reason for the effect is the increase in turbulence level because of particle interaction for cases when $\Phi_g \geqslant 1$ and the combined effect of increase in turbulence level and local promotion of equivalence ratio because of released volatiles from coal dust for methane–air equivalence ratio less than 1.
2. The turbulent burning velocity increases as particle size decreases and dust concentration increases. This is because of the increase in the turbulence level by particle interaction with the turbulent flow, which also increases with increased number of particles present at higher concentrations. This improves the overall heat and mass transfer and the burning velocity increases.
3. Particles interacting with a fuel lean methane–air flame ($\Phi_g < 1$) show the highest increase in the turbulent burning velocity because of an increase in the local equivalence ratio caused by the particle volatization.
4. An empirical correlation of the form $\frac{S_{T,st}}{S_{L,st}} = 1 + C \left(\frac{u'_{rms}}{S_{L,st}} \right)^n$, can correlate the experimental data. The exponent $n = 0.2$. $C = 2.2$ (fuel lean) and $C = 1.7$ (fuel rich).

References

[1] W.L. Frank, M.L. Holcomb, Housekeeping Solutions, Symposium on Dust Explosion Hazard Recognition and Control: New Strategies, Baltimore, Maryland, 2009.
[2] P.R. Amyotte, K.J. Mintz, M.J. Pegg, Y.H. Sun, K.I. Wilkie, J. Loss Prev. Process Ind. 4 (1991) 102–109.
[3] D. Bradley, Z. Chen, S. El-Sherif, S. El-Din Habik, G. John, Combust. Flame 96 (1994) 80–96.
[4] W. Ju, R. Dobashi, T. Hirano, J. Loss Prev. Process Ind. 11 (1998) 177–185.
[5] M.G. Andac, F.N. Egolfopoulos, C.S. Cambell, R. Lauvergne, Proc. Combust. Inst. 28 (2000) 2921–2929.
[6] R. Pilao, E. Ramalho, C. Pinho, J. Loss Prev. Process Ind. 19 (2006) 17–23.
[7] A. Garcia-Agreda, A. Di Benedetto, P. Russo, E. Salzano, R. Sanchirico, Powder Technol. 205 (2011) 81–86.
[8] P. Russo, A. Di Benedetto, R. Sanchirico, Chem. Eng. Trans. 26 (2012).
[9] Y. Liu, J. Sun, D. Chen, J. Loss Prev. Process Ind. 20 (2007) 691–697.
[10] R.K. Eckhoff, Dust Explosions in the Process Industries, Gulf Professional Publishing, Boston, 2003.
[11] H. Kobayashi, T. Tamura, K. Maruta, T. Niioka, F.A. Williams, Proc. Combust. Inst. 26 (1996) 389–396.
[12] M.R. Khan, R.G. Jenkins, Fuel 64 (2) (1985) 189–192.
[13] R. Liu, D.S.K. Ting, G.W. Rankin, Exp. Thermal Fluid Sci. 28 (2004) 307–316.
[14] P.E. Roach, Heat and Fluid Flow 8 (1987) 82–92.
[15] S.R. Rockwell, Influence of Coal Dust on Premixed Turbulent Methane–air Flames, PhD thesis, Fire Protection Engineering, Worcester Polytechnic Institute, 2012.
[16] H.H. Bruun, Hot-wire Anemometry: Principles and Signal Analysis, Oxford University Press, USA, 1995. p. 64.
[17] J.H. Grover, E.N. Fales, A.C. Scurlock, Proc. Combust. Inst. 9 (1963) 21–35.
[18] N. Peters, Proc. Combust. Inst. 21 (1986) 1231–1250.
[19] S.R. Turns, An Introduction to Combustion: Concepts and Applications, McGraw Hill, New York, 2000.
[20] C. Crowe, M. Sommerfeld, Y. Tsuji, Multiphase Flows with Droplets and Particles, CRC Press, Boston, 1998.
[21] R.A. Gore, C.T. Crowe, Int. J. Multiphase Flow 15 (1989) 279–285.
[22] C.T. Crowe, Int. J. Multiphase Flow 26 (2000) 719–727.
[23] Y. Xie, V. Raghavan, A.S. Rangwala, Combust. Flame 159 (2012) 2449–2456.
[24] D. Bradley, M. Lawes, H.Y. Park, N. Usta, Combust. Flame 144 (2006) 190–204.